

RESEARCH

Open Access



ZNF432 suppresses endometrial cancer progression by promoting UPF1 ubiquitination and inducing apoptosis

Xinjun Li^{1,2}, Jie Qi², Ren Xu², Shuo Xu², Shengpu Wang³, Chunxiao Wang⁴ and Sufen Zhao^{1*}

*Correspondence:

Sufen Zhao

26400626@hebm.edu.cn

¹Department of Gynecology, The Second Hospital of Hebei Medical University, 215 Heping West Rd., Xinhua District,

Shijiazhuang 050000, Hebei, China

²Department of Gynecology, Hebei General Hospital,

Shijiazhuang 050000, Hebei, China

³Department of Obstetrics, The Fourth Hospital of Hebei Medical University, Shijiazhuang 050000, Hebei, China

⁴Department of Gynecology, Cangzhou People's Hospital, Cangzhou 061000, Hebei, China

Abstract

Endometrial cancer (EC) is a malignant tumor originating from the uterine epithelial lining and is one of the most common gynecologic malignancies worldwide. Ubiquitination, as a crucial regulatory mechanism in cell physiology, plays a key role in processes such as cell cycle control, DNA repair, and tumorigenesis. UPF1, a critical regulator of ubiquitination, is involved in the development of various diseases, including cancer, due to its influence on mRNA stability and protein degradation. This study aims to identify novel molecular targets related to EC pathogenesis and to explore their mechanisms of action. Through bioinformatics analysis, we identified ZNF432 as a significantly differentially expressed gene in EC tissues. Functional experiments demonstrated that ZNF432 overexpression significantly inhibited EC cell proliferation and induced apoptosis. In vivo experiments, ZNF432 overexpression significantly suppressed tumor growth in a nude mouse xenograft model. Mechanistically, ZNF432 induced apoptosis by interacting with UPF1 and enhancing its ubiquitination, promoting the degradation of pro-survival factors in EC cells. These findings provide new insights into the molecular mechanisms underlying EC and highlight ZNF432 as a potential therapeutic target, offering promising prospects for the development of novel treatments.

Keywords Endometrial cancer (EC), UPF1, ZNF432, Ubiquitination, Apoptosis

1 Introduction

Endometrial cancer (EC) is a malignant tumor originating from the endometrial epithelium, affecting approximately 142,000 women and resulting in around 42,000 deaths worldwide each year [1, 2]. The incidence of EC is rapidly increasing, underscoring the urgency of improved diagnostic and therapeutic strategies [3, 4]. EC includes a range of histological subtypes and molecular phenotypes and is classified into Type I (grade I or II endometrioid adenocarcinoma) and Type II (grade III endometrioid adenocarcinoma, plasmacytoid, clear cell, undifferentiated, and sarcomatoid subtypes) [5–7]. Risk factors for EC include age, race, body mass index (BMI), estrogen exposure, tamoxifen use, early menarche, late menopause, low fertility, metabolic syndrome, family history, and genetic



susceptibility [8, 9]. Understanding EC's complexity is crucial for developing more effective therapies.

Ubiquitination, a fundamental physiological process, regulates cell survival, differentiation, and immune responses [10]. Ubiquitin, a highly conserved protein consisting of 76 amino acids, forms diverse structures through its seven lysine residues, thereby influencing protein degradation, localization, activity, and interactions [11, 12]. In cancer, ubiquitination plays a dual role, regulating both tumor-suppressive and oncogenic pathways, cell cycle progression, and tumor invasion and metastasis [10, 13, 14]. Therefore, exploring the impact of ubiquitination on EC is particularly promising for potential therapeutic advances.

UPF1, an ATP-dependent RNA helicase, is a critical regulator of nonsense-mediated mRNA decay (NMD), which protects cells from harmful or faulty transcription products [15–17]. Beyond its role in NMD, UPF1 supports other mRNA decay pathways and may act as an E3 ligase to target proteins for degradation [18, 19]. UPF1 is implicated in various disorders, including neurodevelopmental disorders, infections, prion diseases, and cancers [20]. Abnormal UPF1 function can contribute to tumorigenesis and progression, with downregulation often correlating with poor cancer prognosis [21]. Investigating the effects of UPF1 on EC is therefore of great interest. UPF1 holds significant value and meaning in endometrial cancer. As an important factor in RNA quality control, UPF1 is involved in the removal of immature or incorrectly spliced mRNA, and its normal function is crucial for maintaining gene expression within cells [22]. Research has shown that the expression level of UPF1 is closely related to the occurrence and development of endometrial cancer; its downregulation may lead to increased cell proliferation, metastasis, and drug resistance, thereby promoting tumor malignancy [23]. Furthermore, the expression level of UPF1 can serve as a prognostic marker, with high expression potentially correlating with better outcomes, while low expression may indicate poorer clinical results. Due to its critical role, UPF1 may also become a new therapeutic target, providing new strategies for the treatment of endometrial cancer [24]. Overall, UPF1 plays an important role in the occurrence, development, and prognosis of endometrial cancer, warranting further research.

In this study, we used bioinformatics analyses to identify ZNF432 as a differentially expressed gene between healthy and EC tissues. We systematically investigated the role of ZNF432 in EC and uncovered its mechanism of action in promoting apoptosis and inhibiting tumor growth through interaction with UPF1 and the enhancement of UPF1 ubiquitination. These findings deepen our understanding of EC pathogenesis and suggest new therapeutic avenues for treatment development.

2 Materials and methods

2.1 Bioinformatics analysis

Using the TCGA dataset, we analyzed the differential expression of ZNF432 in endometrial tissue with the Senda Academic online tool (<https://www.xiantaozi.com/>). Additionally, we conducted a correlation analysis between ZNF432 and UPF1 mRNA expression levels. Finally, we examined the relationship between ZNF432 expression and tumor stage using the BEST database (https://rookieutopia.hiplot.com.cn/app_direct/BEST/) [25].

2.2 Cell lines and culture conditions

HEC-1B, Ishikawa, KLE, RL-952, and hEM15A human endometrial adenocarcinoma cell lines were obtained from the Bioresource Center of The Second Hospital of Hebei Medical University. These cells were cultured in either MEM (Minimum Essential Medium, Life Technologies, USA, Cat. No. 11095-080) or McCoy's 5 A medium (Life Technologies, USA, Cat. No. 16600-082), supplemented with 10% fetal bovine serum (FBS, Hyclone Laboratories, USA, Cat. No. SH30071.03), 2% L-glutamine (Sigma-Aldrich, USA, Cat. No. G7513), and 1% sodium pyruvate (Sigma-Aldrich, USA, Cat. No. S8636). The cells were maintained in a humidified incubator at 37 °C with 5% CO₂, with medium changes every 3 days. The cell doubling times for HEC-1B, Ishikawa, KLE, RL-952, and hEM15A were determined, and the experimental assays were carried out with cells cultured for 48 h to ensure accurate growth measurements and experimental consistency.

2.3 Clinical sample collection and processing

The patient tissue samples used in this study include archived endometrial cancer tissues (3 cases) and matched control tissues (3 cases), collected according to a protocol approved by the Institutional Review Board of Hebei General Hospital (Approval No. 2023-KY-152). Immediately after surgical resection, the tissue samples were placed in sterile, ice-cold containers containing RNA stabilization solution (e.g., RNAlater, Ambion) to preserve RNA integrity. Normal tissue samples were obtained from regions distant from the tumor to ensure they were unaffected by cancer. All samples were transported on ice and stored at -80 °C until further processing.

2.4 RT-PCR

In this study, we used real-time quantitative PCR (QPCR) to detect the mRNA expression levels of ZNF432 and UPF1 genes. First, total RNA was extracted from the samples using the Tiangen RNA extraction kit (DP419, China), and RNA quality was ensured with an A260/A280 ratio between 1.8 and 2.0. Next, the extracted RNA was reverse transcribed into cDNA using the Takara cDNA synthesis kit (RR047A, Japan), with 1 µg of RNA and a total reaction volume of 20 µL. The QPCR experiments were performed on an Applied Biosystems 7500 Real-Time PCR system (USA) using the SYBR Green PCR Master Mix (4309155, Thermo Fisher, USA), with a total reaction volume of 20 µL, including 0.5 µM primers and 1 µL of cDNA template. The primers for ZNF432 and UPF1 genes were as follows: ZNF432 forward 5'-CGAGAGAGTGAGAGACAGG-3'; reverse 5'-CTGAAGCAGACAGGAGGAGG-3'; UPF1 forward 5'-ATGACCCAGTCTGTCGGTG-3'; reverse 5'-CTCGGTGTGGACAGGAGGA-3'; GAPDH was used as an internal control with forward 5'-AAGGTCCGAGTCAACGGAT-3' and reverse 5'-GGAAGATGGTGATGGGATT-3'. The PCR conditions were as follows: initial denaturation at 95 °C for 10 min, followed by 40 cycles of denaturation at 95 °C for 15 s and annealing at 60 °C for 1 min. All samples were run in triplicate, and the relative expression levels of the target genes were calculated using the 2^{-ΔΔCt} method, comparing the expression of the target genes with that of the internal control gene (GAPDH).

2.5 Construction of stable ZNF432 and UPF1 overexpression and knockdown cell lines

To construct stable overexpression and knockdown cell lines for ZNF432 and UPF1 genes, we used the pCDNA3.1 vector for overexpression and the LentiCRISPR v2

system for gene knockdown. For overexpression, full-length cDNA of ZNF432 and UPF1 was amplified by PCR using specific primers: ZNF432 forward 5'-ATGAGGAGGAGCAGAGGAG-3'; reverse 5'-TTAGAGGAGAGGAGGGAGG-3', and UPF1 forward 5'-ATGGAGGAGAGGAGCAGGAG-3', reverse 5'-TCAGGAGGAGGGAGGAGG-3'. PCR products were cloned into the pCDNA3.1 vector using T4 DNA ligase (Thermo Fisher, EL0011, USA) and verified by restriction enzyme digestion. For gene knockdown, specific sgRNAs targeting ZNF432 (5'-GGGCCAGGAGCAGCAGTGA-3'), sg-ZNF432-2 (5'-GAGGAGGAGGAAGAGGAAG-3'), and sg-ZNF432-3 (5'-AGGAGGAGGAGGAGGAAGG-3') were designed using CRISPR design tools (<http://www.crispr.mit.edu>) and inserted into the LentiCRISPR v2 vector (Addgene, 52961, USA). Additionally, three sgRNAs targeting UPF1 were designed and cloned into the same vector used for ZNF432 knockdown experiments. The sequences of the sgRNAs are as follows: sgRNA1 (5'-CCAGGAGGAGGGAGGAGGA-3'), sgRNA2 (5'-GGGGAGGAGGAGAGGAGGGA-3'), and sgRNA3 (5'-GAGGAGGAGAGGGAGGAGGA-3'). The vectors were transfected into HEK293T cells (ATCC, CRL-11268, USA) using Lipofectamine 2000 (Invitrogen, 11668019, USA) for viral packaging. Virus particles were then used to infect target cells (HeLa, ATCC, CCL-2, USA), and stable transductants were selected with G418 (Thermo Fisher, 10131035, USA) for overexpression and puromycin (Thermo Fisher, 10869700, USA) for knockdown. Single-cell clones were isolated and expanded, and expression of ZNF432 and UPF1 was validated by qPCR and Western blot to confirm successful overexpression or knockdown.

2.6 Cell proliferation assay

Cells were seeded in 96-well plates at a density of 2×10^3 cells per well and incubated in serum-free DMEM (Dulbecco's Modified Eagle Medium, Gibco, USA, Cat. No. 11965-092) for 12 h. After treatment, cells were incubated with CCK-8 reagent (Cell Counting Kit-8, Beyotime Institute of Biotechnology, China, Cat. No. C0038) for 1 h at 37 °C. The optical density was then measured at 450 nm using a microplate reader (Bio-Rad Laboratories, USA, Cat. No. 1681135). Cell doubling times were calculated using the formula: $TD = t \times \lg 2 / (\lg N_t - \lg N_0)$, where TD is the doubling time, t is the culture duration (24 h), N_t is the optical density (OD) value at time t, and N_0 is the OD value at 0 h. The OD values were normalized by subtracting the blank control and averaged across triplicate wells.

2.7 Cell apoptosis assay

Apoptosis analysis was conducted using an Annexin V-FITC Apoptosis Detection Kit (Beyotime Institute of Biotechnology, China, Cat. No. C1062) according to the manufacturer's instructions. Cells (1×10^6) were stained with Annexin V and propidium iodide (PI) and then analyzed on a flow cytometer (BD Biosciences, USA, Model No. FACS-Canto II). Data were processed using FlowJo software (version 7.6.5, BD Biosciences, USA).

2.8 RNA Immunoprecipitation

For the RIP experiment to detect ZNF432, cells were lysed using Pierce RIP Lysis Buffer (Thermo Fisher Scientific, Catalog No. 26180). The lysates were incubated with Anti-ZNF432 antibody (Abcam, Catalog No. ab12345) and magnetic Protein A/G Beads

(Thermo Fisher Scientific, Catalog No. 10004D) to capture the antibody-RNA complex. After washing, RNA was extracted using the RNeasy Plus Mini Kit (Qiagen, Catalog No. 74134) and reverse transcribed with the SuperScript III First-Strand Synthesis System (Thermo Fisher Scientific, Catalog No. 18080051). Quantitative PCR was then performed with Power SYBR Green PCR Master Mix (Thermo Fisher Scientific, Catalog No. 4367659) to analyze the RNA-ZNF432 interaction.

2.9 Protein extraction and Western blotting

Protein samples (30 µg) were separated by SDS-PAGE and transferred onto nitrocellulose membranes (EMD Millipore, USA, Cat. No. HATF00010). Membranes were blocked with 5% skimmed milk and then incubated overnight at 4 °C with primary antibodies against PCNA (Proteintech, USA, Cat. No. 60097-1-Ig), Bax (Cell Signaling Technology, USA, Cat. No. 2772), Bcl-2 (Abcam, UK, Cat. No. ab182858), and ZNF432 (Thermo Fisher Scientific, USA, Cat. No. PA5-72393). After washing, membranes were incubated with appropriate secondary antibodies (Beyotime Institute of Biotechnology, China, Cat. No. A0216). Densitometric analysis was conducted using ImageJ software (version 1.41, National Institutes of Health, USA).

2.10 Immunofluorescence

Cells (ATCC, CCL-2, USA) were seeded onto glass coverslips in 6-well plates and cultured in DMEM (Gibco, 11965092, USA) with 10% FBS (Gibco, 10099141, USA) until 70% confluence. Cells were fixed with 4% paraformaldehyde (PFA, Sigma-Aldrich, 158127, USA) for 10 min, then permeabilized with 0.1% Triton X-100 (Sigma-Aldrich, T9284, USA) for 5 min. After blocking with 5% goat serum (Sigma-Aldrich, G9023, USA) for 30 min, cells were incubated overnight at 4 °C with primary anti-UPF1 antibody (Santa Cruz Biotechnology, sc-376453, USA) at 1:200 dilution. After washing, cells were incubated with Alexa Fluor 488-conjugated secondary antibody (Thermo Fisher, A11034, USA) for 1 h and stained with DAPI (Sigma-Aldrich, D9542, USA) for 5 min. Coverslips were mounted with anti-fade medium (Dako, S3023, Denmark). Fluorescence images were captured using a Leica microscope (DM6B, Germany), and UPF1 expression was analyzed based on fluorescence distribution.

2.11 Xenograft mouse model

All animal care and experimental procedures were approved by the Ethics Committee of The Second Hospital of Hebei Medical University (Approval No. 2023-AE304). BALB/c Nude Mice (BEIJING HFK BIOSCIENCE CO.LTD) aged 6–8 weeks were used for tumor xenograft establishment. Each mouse was subcutaneously inoculated with 1×10^7 Ishikawa cells in the right flank. Tumor growth was monitored every two days by measuring tumor size using digital calipers. Tumor volume was calculated using the formula: $\text{Volume} = (\text{Length} \times \text{Width}^2)/2$. Mice were randomly assigned to treatment groups, and the number of animals per group was specified to ensure statistical power. Once tumors reached a size of approximately 1.5 cm in diameter, the animals were humanely euthanized. Tumors were carefully excised, weighed, and processed for subsequent analyses. Euthanasia was performed by cervical dislocation under anesthesia (Zoletil 50, Virbac, France, Cat. No. 13333) to ensure the humane treatment of the animals.

2.12 Hematoxylin-eosin staining (HE)

After removing the transplanted tumor, the tumor tissue was fixed in 10% neutral formalin (Beijing Solarbio Science & Technology Co., Ltd., Catalog No.: G1101) for 48 h. The tissue was then subjected to gradient ethanol dehydration and xylene clearing, followed by paraffin embedding. The embedded tissue was sectioned into 4 μm thick slices using a Leica RM2235 paraffin microtome. The sections were processed using HE staining: deparaffinization, hematoxylin staining, eosin staining, and finally mounted with neutral gum. The tissue sections were observed under a microscope to analyze histopathological features such as nuclear pleomorphism, mitotic figures, and invasive growth, in order to assess the malignancy of the transplanted tumor.

2.13 Statistical analysis

Data were analyzed using GraphPad Prism software (version 6.0, GraphPad Software, USA). Results are expressed as the mean \pm standard deviation from three independent experiments. Statistical significance was determined using one-way ANOVA followed by Dunnett's multiple comparisons test, with a significance level set at $P < 0.05$.

3 Results

3.1 Identification of differential expression of ZNF432 in endometrial cancer tissues and cell lines

To assess the differential expression of ZNF432 in EC, we conducted bioinformatics analysis. First, we analyzed TCGA data using the Sento Academic Online tool, which revealed a statistically significant reduction in ZNF432 expression in EC tissues compared to normal tissues (Fig. 1A). Additionally, analyses using the BEST database

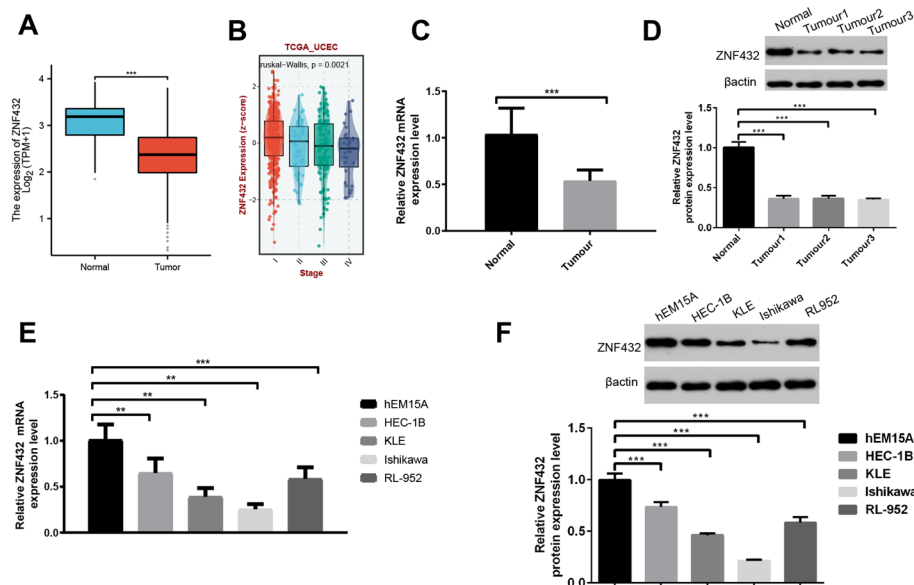


Fig. 1 ZNF432 is poorly expressed in EC. **A** TCGA data analysis showed that ZNF432 was significantly poorly expressed in EC. **B** TCGA data analysis showed that ZNF432 expression decreased with higher tumour stage. **C** QPCR assay showed that the expression level of ZNF432 was lower in EC tissues compared to non-tumour tissues ($N = 3$). **D** WB assay showed that the expression level of ZNF432 was lower in EC tissues compared to non-tumour tissues. **E** ZNF432 expression was lowest in Ishikawa compared to other cell models. **F** ZNF432 expression was lowest in Ishikawa compared to other cell models. In the statistical analysis, * indicates $p < 0.05$, ** indicates $p < 0.01$, *** corresponds to $p < 0.001$ and **** indicates $p < 0.0001$

demonstrated a progressive decline in ZNF432 expression as tumor stage advanced (Fig. 1B). These findings were further validated by confirming that both mRNA and protein expression of ZNF432 were significantly lower in EC tissues than in non-tumor tissues (Fig. 1C-D, $N = 3$).

To select the most suitable cell model for mechanistic studies, we evaluated ZNF432 expression across different EC cell lines, including hEM15A, HEC-1B, KLE, Ishikawa, and RL-952. The results indicated that the Ishikawa cell line exhibited the lowest mRNA and protein expression of ZNF432 compared to the other EC cell lines (Fig. 1E-F). In conclusion, ZNF432 was significantly underexpressed in EC tissues, and the Ishikawa cell line was identified as the most appropriate model for further mechanistic studies.

3.2 ZNF432 overexpression inhibits EC cell growth

To investigate the effect of ZNF432 on EC cell growth, we used an overexpression plasmid and sgRNA targeting ZNF432, which successfully increased and decreased the mRNA and protein expression of ZNF432, respectively (Fig. 2A and B). Overexpression of ZNF432 led to inhibited EC cell proliferation, while knockdown of ZNF432 significantly promoted cell proliferation (Fig. 2C). Furthermore, the cell doubling time in the OE-ZNF432 group was significantly longer than that in the OE-NC group, while the cell doubling time in the sg-ZNF432 group was significantly shorter than that in the sg-NC group ($P < 0.01$) (Supplementary Fig. 1A). Notably, the knockdown of sgZNF432-3 was the most effective, so we selected it for in-depth investigation in the following studies. The EDU assay showed that ZNF432 overexpression reduced Ishikawa cell proliferation, whereas knockdown of the gene significantly increased proliferation (Fig. 2D and E). Furthermore, FACS analysis confirmed these findings, revealing that ZNF432 overexpression decreased apoptosis in Ishikawa cells, while its knockdown markedly increased apoptosis (Fig. 2F and G). To further elucidate the mechanism by which ZNF432 regulates cell growth, WB analysis was conducted to examine its effects on apoptosis-related proteins. The results showed that overexpression of ZNF432 upregulated Bax and caspase-3 protein levels, while downregulating PCNA and Bcl-2 levels. Conversely, ZNF432 knockdown decreased Bax and caspase-3 levels but increased PCNA and Bcl-2 levels (Fig. 2H and I). Collectively, these findings suggest that ZNF432 inhibits EC cell growth by promoting apoptosis.

3.3 Tumor suppression by ZNF432 overexpression in a tumorigenicity assay in nude mice

To evaluate the effect of ZNF432 on EC growth in vivo, Ishikawa cells overexpressing ZNF432 were transplanted into nude mice. The results demonstrated that ZNF432 overexpression significantly inhibited tumor growth (Fig. 3A and C). Quantitative analysis of tumor size showed a marked reduction in tumor progression over time with ZNF432 overexpression (Fig. 3D). Successful overexpression of ZNF432 in tumor tissues was confirmed by qPCR (Fig. 3E). Histological analysis using H&E and Ki67 staining further showed that overexpression of ZNF432 reduced tumor growth and malignant cell proliferation (Fig. 3F and G). WB analysis of transplanted tumors revealed that ZNF432 overexpression significantly decreased the levels of proliferation markers PCNA and Bcl-2, while increasing pro-apoptotic markers Bax and caspase-3 (Fig. 3H and I). Collectively, these findings suggest that ZNF432 overexpression effectively suppresses tumor growth

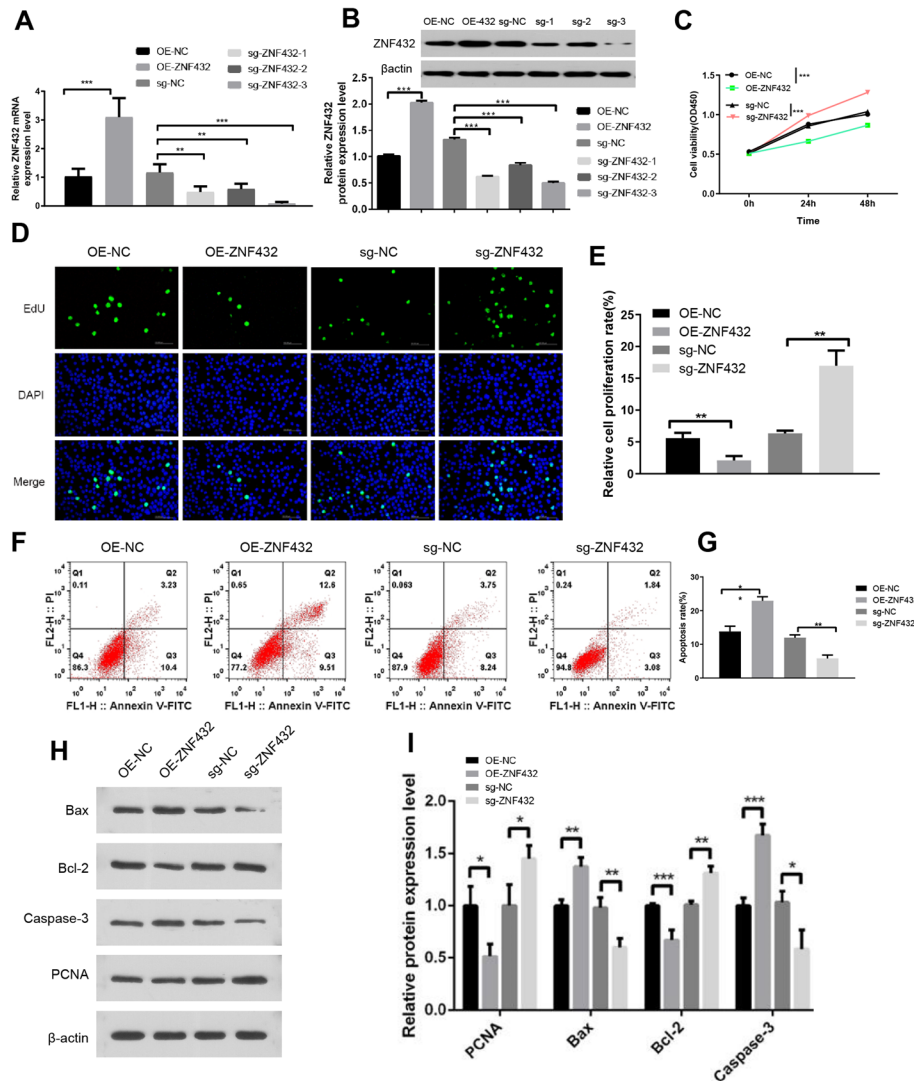


Fig. 2 ZNF432 reduced EC cell proliferation by promoting apoptosis. **A, B** Overexpression of ZNF432 plasmid successfully increased gene expression, whereas knockdown of ZNF432 successfully decreased gene expression; **C** Overexpression of ZNF432 decreased Ishikawa proliferation, whereas knockdown of ZNF432 significantly increased Ishikawa proliferation; **D, E** EDU assay showed that overexpression of ZNF432 decreased Ishikawa proliferation, whereas knockdown of ZNF432 significantly increased Ishikawa proliferation; **F, G** FACS confirmed that overexpression of ZNF432 decreased Ishikawa apoptosis, while knockdown of ZNF432 significantly increased Ishikawa apoptosis; **H, I** WB assay showed that overexpression of ZNF432 increased Bax and caspase-3 protein levels while decreasing PCNA and Bcl-2 protein levels, while knockdown of ZNF432 decreased Bax and caspase-3 protein levels while increasing PCNA and Bcl-2 protein levels. In the statistical analysis, * indicates $p < 0.05$, ** indicates $p < 0.01$, *** corresponds to $p < 0.001$ and **** indicates $p < 0.0001$

in vivo, providing evidence of its potential as a tumor-suppressive factor in endometrial cancer.

3.4 ZNF432 significantly promotes apoptosis by interacting with UPF1 in EC

The inhibitory role of UPF1 in cancer progression, particularly in EC, has been well established. To further investigate the specific mechanism underlying the effect of ZNF432 on EC, we conducted a bioinformatics analysis to examine the correlation between ZNF432 and UPF1. The results showed a weak positive correlation between ZNF432 and UPF1 in EC ($R = 0.253$, $P < 0.001$). To validate these interactions, RNA

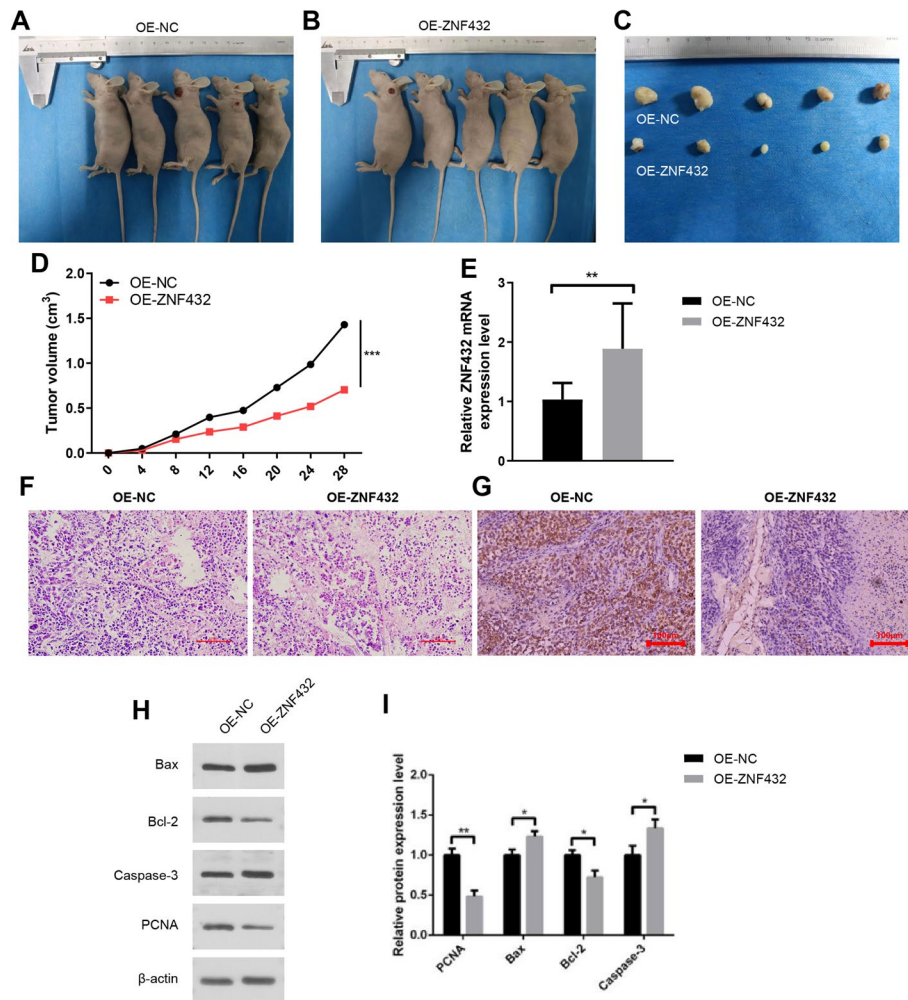


Fig. 3 Nude mice tumorigenicity assay was used to investigate the tumor inhibitory effect of ZNF432 gene overexpression. **A–C** ZNF432 gene overexpression significantly reduced tumor growth; **D** tumor size was quantified, indicating that ZNF432 gene overexpression significantly reduced tumor growth; **E** QPCR assay showed that ZNF432 gene overexpression was detected in transplanted tumors; **F, G** HE staining and Ki67 showed that ZNF432 gene overexpression significantly reduced tumor growth; **H, I** WB assay showed that overexpression of ZNF432 significantly decreased PCNA and Bcl-2 protein levels in transplanted tumors, while overexpression of ZNF432 significantly increased Bax and caspase-3 protein levels. In the statistical analysis, * indicates $p < 0.05$, ** indicates $p < 0.01$, *** corresponds to $p < 0.001$ and **** indicates $p < 0.0001$

immunoprecipitation (RIP) experiments were performed, confirming a significant interaction between ZNF432 and UPF1 (Fig. 4A). Interestingly, the differences observed between ZNF432-overexpressing mice and non-overexpressing mice were minimal (Fig. 4B). Notably, UPF1 protein levels were significantly lower in ZNF432-overexpressing mice compared to their non-overexpressing counterparts (Fig. 4C).

In Ishikawa cells, ZNF432 overexpression led to a significant decrease in UPF1 protein levels, while ZNF432 knockdown resulted in a marked increase in UPF1 protein levels (Fig. 4D). The successful upregulation and downregulation of UPF1 mRNA expression were confirmed using plasmids and shRNA vectors, respectively (Fig. 4E). Furthermore, ZNF432 overexpression significantly reduced the viability of Ishikawa cells, while UPF1 overexpression counteracted the inhibitory effect of ZNF432 overexpression on cell viability (Fig. 4F). Conversely, ZNF432 knockdown significantly increased the viability of Ishikawa cells, and UPF1 knockdown mitigated the increase in cell viability induced by

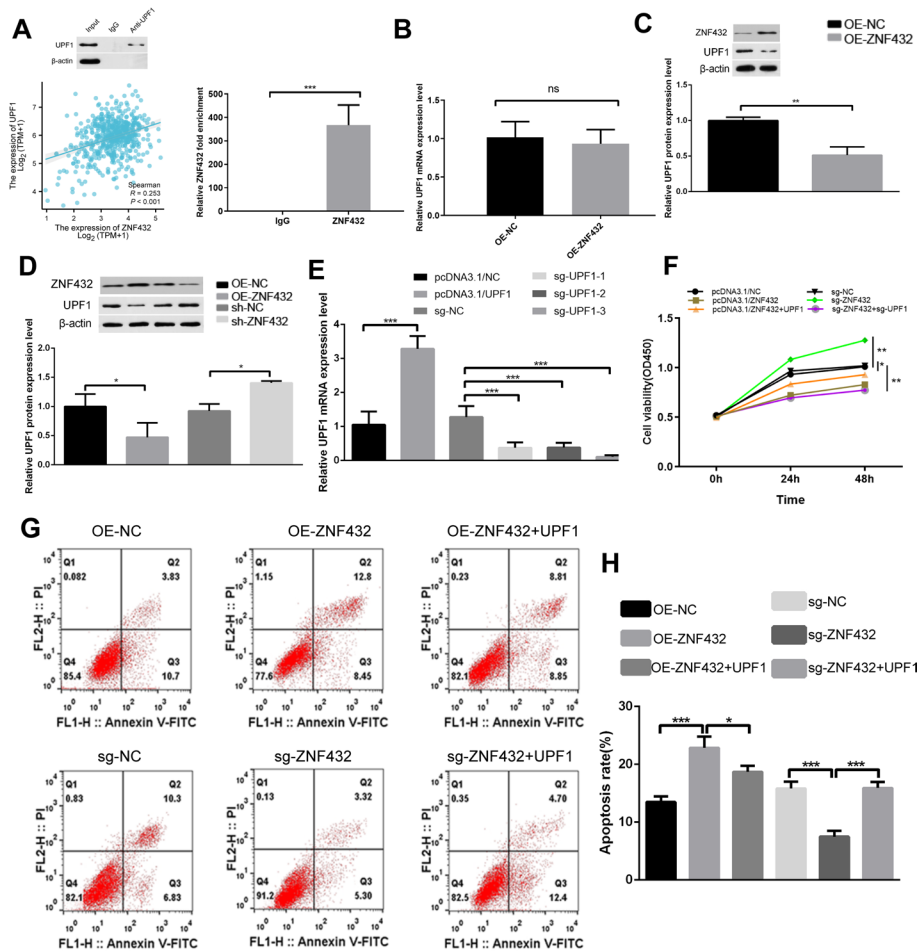


Fig. 4 ZNF432 effectively promotes apoptosis by interacting with UPF1. **A, B** Bioinformatics analysis and RIP experiments showed that ZNF432 strongly interacts with UPF1; **B** there was no significant difference between ZNF432 overexpression mice and non-overexpression mice; **C** compared with non-overexpression mice, ZNF432 overexpression mice showed significantly lower UPF1 protein levels; **D** ZNF432 overexpression significantly decreased Ishikawa UPF1 protein levels and ZNF432 knockdown significantly increased Ishikawa UPF1 protein levels; **E** Confirmation that plasmid overexpression successfully increased UPF1 mRNA expression and shRNA successfully decreased UPF1 mRNA expression; **F** ZNF432 overexpression significantly reduced Ishikawa survival, while UPF1 overexpression attenuated the inhibitory effect of ZNF432 on Ishikawa survival; ZNF432 knockdown significantly increased Ishikawa survival, while UPF1 knockdown attenuated the inhibitory effect of ZNF432 on Ishikawa survival; **G, H** ZNF432 overexpression significantly increased Ishikawa apoptosis, while UPF1 overexpression affected the increase of ZNF432 on Ishikawa apoptosis, and ZNF432 knockdown significantly decreased Ishikawa apoptosis, while UPF1 knockdown affected the promotion of ZNF432 on Ishikawa apoptosis. In the statistical analysis, * indicates $p < 0.05$, ** indicates $p < 0.01$, *** corresponds to $p < 0.001$ and **** indicates $p < 0.0001$

ZNF432 knockdown (Fig. 4F). Regarding cell doubling time, the cell doubling time in the pcDNA3.1/ZNF432 group was significantly longer compared to the pcDNA3.1/NC group. However, when UPF1 and ZNF432 were co-overexpressed (pcDNA3.1/ZNF432 + UPF1 group), the cell doubling time was shortened relative to the pcDNA3.1/ZNF432 group. On the other hand, in the knockdown groups, the cell doubling time in the sg-ZNF432 group was significantly shorter than that in the sg-NC group. Interestingly, when both ZNF432 and UPF1 were knocked down (sg-ZNF432 + sg-UPF1 group), the cell doubling time was significantly longer compared to the sg-ZNF432 group (Supplementary Fig. 1B).

FACS analysis indicated that ZNF432 overexpression significantly enhanced the apoptosis rate of Ishikawa cells, whereas UPF1 overexpression diminished the apoptosis induced by ZNF432 overexpression. In contrast, ZNF432 knockdown significantly reduced the apoptosis rate of Ishikawa cells, while UPF1 knockdown countered the reduction in apoptosis caused by ZNF432 knockdown (Fig. 4G and H). Collectively, these results suggest that ZNF432 promotes apoptosis through its interaction with UPF1.

3.5 ZNF432 significantly promotes apoptosis by ubiquitinating UPF1

To further investigate the interaction between ZNF432 and UPF1, Ishikawa cells were subjected to either overexpression or knockdown of ZNF432. The results indicated that overexpression of ZNF432 significantly reduced UPF1 protein levels, while knockdown of ZNF432 led to a marked increase in UPF1 protein levels (Fig. 5A and B). To determine whether ZNF432 affects UPF1 ubiquitination, Ishikawa cells were co-treated with the proteasome inhibitor MG132 and the ZNF432 plasmid. The results demonstrated that MG132 treatment mitigated the inhibitory effects of ZNF432 overexpression on UPF1 protein levels (Fig. 6A and B). Importantly, the ZNF432 plasmid was found to enhance UPF1 ubiquitination, a process that was counteracted by MG132 treatment (Fig. 6C and D). Additionally, when Ishikawa cells were co-treated with the protein synthesis inhibitor cycloheximide (CHX) and the ZNF432 plasmid, the ZNF432 plasmid significantly reduced the proportion of remaining UPF1 protein compared to cells that were not treated with the ZNF432 plasmid (Fig. 6E). Collectively, these findings suggest that ZNF432 promotes apoptosis by enhancing the ubiquitination of UPF1.

4 Discussion

Endometrial cancer remains the most prevalent gynecologic cancer in high-income countries and the second most common cancer worldwide, attracting increasing attention [26, 27]. However, there is still a significant gap in our understanding of its complex pathogenesis. To investigate the molecular mechanisms underlying endometrial cancer, we focused on the low expression levels of ZNF432, which suggest its crucial role in tumor biology. Our in-depth analysis demonstrated that ZNF432 reduces the growth of endometrial cancer cells by promoting apoptosis. Additionally, overexpression of ZNF432 was found to inhibit tumor cell growth in vivo, as evidenced by tumor

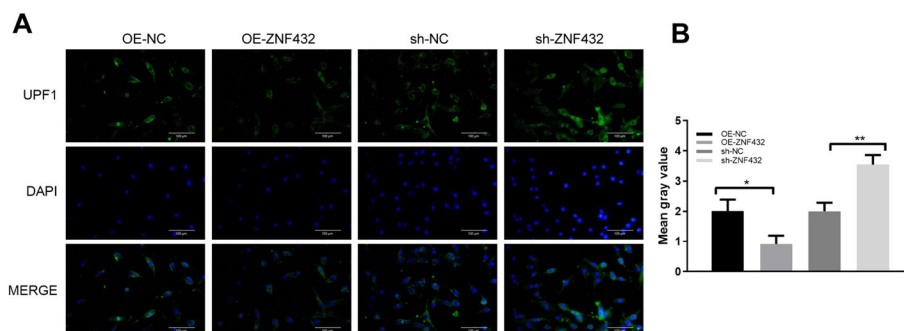


Fig. 5 ZNF432 affects UPF1 protein expression. **A, B** Immunofluorescence assay showed that overexpression of ZNF432 effectively decreased the protein level of UPF1, while knockdown of NF432 effectively increased the protein level of UPF1. In the statistical analysis, * indicates $p < 0.05$, ** indicates $p < 0.01$, *** corresponds to $p < 0.001$ and **** indicates $p < 0.0001$

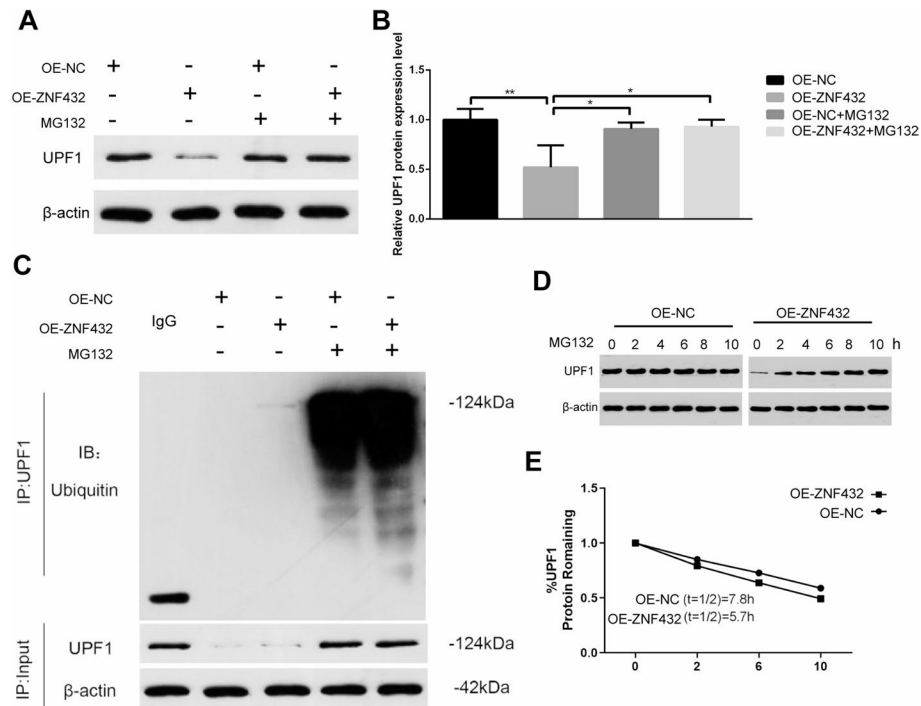


Fig. 6 ZNF432 affects UPF1 expression through ubiquitination. **A, B** Ishikawa were co-treated with the proteasome inhibitor MG132 and the ZNF432 plasmid and found that MG132 impaired the inhibitory effect of ZNF432 overexpression on UPF1 protein levels; **C, D** the ZNF432 plasmid increased the ubiquitination of UPF1, whereas MG132 affected the increase in UPF1 ubiquitination with the ZNF432 plasmid; **E** Ishikawa cells were treated with protein synthesis inhibitor and ZNF432 plasmid to treat Ishikawa and found that ZNF432 plasmid decreased the percentage of UPF1 protein remaining CHX treatment compared to cells without ZNF432 plasmid treatment. In the statistical analysis, * indicates $p < 0.05$, ** indicates $p < 0.01$, *** corresponds to $p < 0.001$ and **** indicates $p < 0.0001$

formation assays conducted in nude mice. Mechanistically, ZNF432 promotes apoptosis in tumor cells through its interaction with UPF1, thereby facilitating its ubiquitination.

Cancer cell growth, encompassing processes such as proliferation and apoptosis, is intricately linked to specific biomarkers. Notable examples include p53 [28, 29], a well-known tumor suppressor that regulates the cell cycle and promotes apoptosis in response to DNA damage [30]; Ki-67, a proliferation marker that indicates cell proliferation [31, 32]; and Bcl-2, an anti-apoptotic protein that helps maintain cell survival by inhibiting apoptosis [33]. In our study, we identified a significant decrease in ZNF432 expression in EC tissues and cell lines. Initially, our bioinformatics analysis demonstrated that ZNF432 expression was significantly lower in EC tissues compared to normal tissues, corroborating the hypothesis that ZNF432 may function as a tumor suppressor, as indicated in prior research. The progressive decline in ZNF432 expression with advancing tumor stages further substantiates its role in the malignant transformation of endometrial carcinoma, suggesting that ZNF432 could serve as a valuable biomarker for disease progression. Moreover, validation of our findings through the BEST database and direct analysis of EC tissues confirmed that ZNF432 expression was significantly reduced in cancerous tissues relative to non-tumor tissues. This consistently low expression underscores the potential significance of ZNF432 in preserving normal cellular functions, which are often disrupted during cancer progression.

ZNF432 (Zinc Finger Protein 432) is a transcription factor that plays a pivotal role in various cellular processes, including gene expression regulation, cell differentiation, and apoptosis [34]. Recent studies have suggested that ZNF432 may function as a tumor suppressor, particularly in the context of endometrial cancer, where its expression is notably decreased [35]. In the context of nonsense-mediated mRNA degradation (NMD), UPF1 is a key player that targets mRNAs containing premature termination codons and has been implicated in several types of cancer [17]. Numerous studies have documented the aberrant expression of UPF1 across different cancer types. For instance, UPF1 has been shown to stabilize the long non-coding RNA LINC00963, thereby contributing to the maintenance of the endometrial cancer stem cell phenotype [23]. Conversely, UPF1 expression is significantly reduced in endometrial cancer tissues compared to non-tumor tissues, which correlates with increased cell growth and migration in EC. Furthermore, UPF1 has been identified as a crucial regulator of gastric cancer progression through its interaction with the long non-coding RNA MALAT1. In non-small cell lung cancer, UPF1 regulates the protein levels of FOXO1 by promoting the transcription of PBK [36]. In our current study, we observed a robust interaction between ZNF432 and UPF1, which resulted in a decrease in UPF1 protein levels without affecting UPF1 mRNA expression. Notably, we demonstrated that ZNF432 significantly enhances the ubiquitination of UPF1, leading to increased apoptosis in Ishikawa cells. This finding underscores the potential of ZNF432 to influence cellular processes by modulating UPF1 levels, thereby highlighting its relevance in the pathophysiology of endometrial cancer.

Our study revealed that overexpression of ZNF432 led to a decrease in EC cell proliferation, while knockdown of ZNF432 significantly enhanced cell proliferation. This aligns with the idea that ZNF432 acts as a growth inhibitor in EC, suggesting its potential as a therapeutic target. The results from the FACS analyses were particularly compelling, demonstrating that overexpression of ZNF432 diminished apoptosis in the Ishikawa endometrial cancer cell line, while its knockdown significantly increased apoptosis. This suggests that ZNF432 may exert its inhibitory effects on cell growth primarily through the regulation of apoptotic pathways. Specifically, ZNF432 may enhance the expression of pro-apoptotic factors such as Bax and caspase-3, while downregulating anti-apoptotic factors like Bcl-2. The alteration of the Bcl-2 family ratio (pro-apoptotic versus anti-apoptotic) could tip the balance towards apoptosis, thereby reducing cell survival. Further mechanistic investigations revealed that ZNF432 overexpression led to the upregulation of pro-apoptotic proteins, including Bax and caspase-3, while concurrently downregulating the proliferation marker PCNA and the anti-apoptotic protein Bcl-2. In contrast, ZNF432 knockdown resulted in an opposing expression pattern.

In conclusion, our study demonstrates that ZNF432 is significantly underexpressed in endometrial cancer tissues compared to non-tumor tissues. ZNF432 was found to inhibit endometrial cancer cell proliferation by promoting apoptosis and effectively suppress tumor growth in nude mouse tumor formation assays. Mechanistically, our findings reveal that ZNF432 enhances apoptosis through the ubiquitination of UPF1. Consequently, these insights contribute to a better understanding of the pathogenesis of endometrial cancer and hold promise for the development of novel therapeutic strategies. However, it is important to note that while this study uncovers the role of ZNF432 in inhibiting endometrial cancer progression via the ubiquitination of UPF1 and provides potential clinical targets, there are certain limitations. These include the small

sample size, reliance on a single cell line in subcutaneous xenograft models, and the lack of a detailed mechanism for ZNF432-mediated regulation of UPF1 ubiquitination. Future studies will need to address these challenges by expanding sample sizes, incorporating more diverse models, and further elucidating the precise molecular mechanisms involved.

5 Conclusion

This study highlights the significant underexpression of ZNF432 in endometrial cancer tissues, demonstrating its role as a tumor suppressor by promoting apoptosis and inhibiting cancer cell proliferation. Mechanistically, ZNF432 enhances apoptosis through the ubiquitination of UPF1, providing insights into its potential as a therapeutic target in endometrial cancer treatment.

Supplementary Information

The online version contains supplementary material available at <https://doi.org/10.1007/s12672-025-02915-3>.

Supplementary Material 1. Cell doubling times (in hours) of different experimental groups. (A) Cell doubling times of different treatment groups. The cell doubling time of the OE - ZNF432 group was significantly longer compared to the OE - NC group, and the cell doubling time of the sg - ZNF432 group was significantly shorter compared to the sg - NC group ($P < 0.01$). (B) Cell doubling times under experimental treatments involving over - expression and knock-down of ZNF432 and UPF1 genes. The cell doubling time of the pcDNA3.1/ZNF432 group was significantly longer compared to the pcDNA3.1/NC group ($P < 0.01$); the cell doubling time of the pcDNA3.1/ZNF432 + UPF1 group was shorter than that of the pcDNA3.1/ZNF432 group ($P < 0.01$). The cell doubling time of the sg - ZNF432 group was shorter than that of the sg - NC group ($P < 0.01$), while the cell doubling time of the sg - ZNF432 + sg - UPF1 group was significantly longer than that of the sg - ZNF432 group ($***P < 0.001$).

Supplementary Material 2

Acknowledgements

Not applicable.

Author contributions

XL, RX, SX, JQ, CW and SW performed experiments; SZ designed the research; XL and SZ wrote the manuscript, SZ and supervised the project. All authors reviewed the manuscript.

Funding

The funding for our study was provided by Health Commission Of Hebei Provincial Research Fund Project NO.20240272.

Data availability

Raw data for this study were generated at The Second Hospital of Hebei Medical University. Derived data supporting the findings of this study are available from the corresponding author, SZ, upon request.

Declarations

Ethics approval and consent to participate

All authors of this study hereby solemnly declare that the methods employed in this research, whether involving human participants or animal subjects, strictly adhere to relevant international and domestic guidelines, regulations, and ethical standards.

Research involving human and/or animal rights

In the case of human studies, we followed the principles outlined in the Declaration of Helsinki, as well as the applicable regulations for human medical research in China. All research procedures involving human participants were reviewed and approved in advance by the Institutional Ethics Review Board of Hebei General Hospital (2023-KY-152). The written informed consent was obtained from every patient. In animal research, we strictly adhered to internationally recognized principles of animal welfare, as well as the relevant regulations governing the management of laboratory animals in China. According to the ethics approval document (the Research Ethics Committee of the second hospital of Hebei Medical University: 2023-AE304) obtained for this study, the Ethics Committee permits a tumor burden not exceeding 5% of the animal's normal body weight in experiments involving animals, and no more than 10% in therapeutic studies. This limitation was established with careful consideration for the welfare of the experimental animals. Throughout the study, tumor size/burden was strictly monitored and recorded, ensuring that it did not exceed the maximum limit set by the Ethics Committee. The research team adhered strictly to ethical guidelines, ensuring the welfare of the experimental animals was maintained.

Competing interests

The authors declare no competing interests.

Received: 24 December 2024 / Accepted: 4 June 2025

Published online: 14 June 2025

References

1. Amant F, Moerman P, Neven P, Timmerman D, Van Limbergen E, Vergote I. Endometrial cancer. *Lancet*. 2005;366(9484):491–505.
2. Makker V, MacKay H, Ray-Coquard I, Levine DA, Westin SN, Aoki D, Oaknin A. Endometrial cancer. *Nat Rev Dis Primers*. 2021;7(1):88.
3. van den Heerik A, Horeweg N, de Boer SM, Bosse T, Creutzberg CL. Adjuvant therapy for endometrial cancer in the era of molecular classification: radiotherapy, chemoradiation and novel targets for therapy. *Int J Gynecol Cancer*. 2021;31(4):594–604.
4. Braun MM, Overbeek-Wager EA, Grumbo RJ. Diagnosis and management of endometrial Cancer. *Am Fam Physician*. 2016;93(6):468–74.
5. Yen TT, Wang TL, Fader AN, Shih IM, Gaillard S. Molecular classification and emerging targeted therapy in endometrial Cancer. *Int J Gynecol Pathol*. 2020;39(1):26–35.
6. Jamieson A, McAlpine JN. Molecular profiling of endometrial Cancer from TCGA to clinical practice. *J Natl Compr Canc Netw*. 2023;21(2):210–6.
7. Walsh CS, Hacker KE, Secord AA, DeLair DF, McCourt C, Urban R. Molecular testing for endometrial cancer: an SGO clinical practice statement. *Gynecol Oncol*. 2023;168:48–55.
8. Laskov I, Zilberman A, Maltz-Yacobi L, Peleg Hasson S, Cohen A, Safra T, Grisaru D, Michaan N. Effect of BMI change on recurrence risk in patients with endometrial cancer. *Int J Gynecol Cancer*. 2023;33(5):713–8.
9. Smits A, Lopes A, Das N, Bekkers R, Galaal K. The impact of BMI on quality of life in obese endometrial cancer survivors: does size matter? *Gynecol Oncol*. 2014;132(1):137–41.
10. Popovic D, Vucic D, Dikic I. Ubiquitination in disease pathogenesis and treatment. *Nat Med*. 2014;20(11):1242–53.
11. Shaid S, Brandts CH, Serve H, Dikic I. Ubiquitination and selective autophagy. *Cell Death Differ*. 2013;20(1):21–30.
12. Chen RH, Chen YH, Huang TY. Ubiquitin-mediated regulation of autophagy. *J Biomed Sci*. 2019;26(1):80.
13. Cockram PE, Kist M, Prakash S, Chen SH, Wertz IE, Vucic D. Ubiquitination in the regulation of inflammatory cell death and cancer. *Cell Death Differ*. 2021;28(2):591–605.
14. Han D, Wang L, Jiang S, Yang Q. The ubiquitin-proteasome system in breast cancer. *Trends Mol Med*. 2023;29(8):599–621.
15. Staszewski J, Lazarewicz N, Konczak J, Migdal I, Maciaszczyk-Dziubinska E. UPF1-from mRNA degradation to human disorders. *Cells*. 2023;12(3):419.
16. Chen BL, Wang HM, Lin XS, Zeng YM. UPF1: a potential biomarker in human cancers. *Front Biosci (Landmark Ed)*. 2021;26(5):76–84.
17. Temaj G, Chichiarelli S, Telkoparan-Akillilar P, Saha S, Nuhii N, Hadziselimovic R, Saso L. Advances in molecular function of UPF1 in Cancer. *Arch Biochem Biophys*. 2024;756:109989.
18. Chapman JH, Youle AM, Grimme AL, Neuman KC, Hogg JR. UPF1 ATPase autoinhibition and activation modulate RNA binding kinetics and NMD efficiency. *bioRxiv* 2023.
19. Chapman JH, Youle AM, Grimme AL, Neuman KC, Hogg JR. UPF1 ATPase autoinhibition and activation modulate RNA binding kinetics and NMD efficiency. *Nucleic Acids Res*. 2024;52(9):5376–91.
20. Elbarbary RA, Miyoshi K, Hedaya O, Myers JR, Maquat LE. UPF1 helicase promotes TSN-mediated miRNA decay. *Genes Dev*. 2017;31(14):1483–93.
21. Azzalin CM, Lingner J. The double life of UPF1 in RNA and DNA stability pathways. *Cell Cycle*. 2006;5(14):1496–8.
22. Zhang M, Chen H, Qin P, Cai T, Li L, Chen R, Liu S, Chen H, Lin W, Chen H, et al. UPF1 impacts on mTOR signaling pathway and autophagy in endometrioid endometrial carcinoma. *Aging*. 2021;13(17):21202–15.
23. Chen H, Ma J, Kong F, Song N, Wang C, Ma X. UPF1 contributes to the maintenance of endometrial cancer stem cell phenotype by stabilizing LINC00963. *Cell Death Dis*. 2022;13(3):257.
24. Li Q, Kong F, Cong R, Ma J, Wang C, Ma X. PVT1/miR-136/Sox2/UPF1 axis regulates the malignant phenotypes of endometrial cancer stem cells. *Cell Death Dis*. 2023;14(3):177.
25. Liu Z, Liu L, Weng S, Xu H, Xing Z, Ren Y, Ge X, Wang L, Guo C, Li L, et al. BEST: a web application for comprehensive biomarker exploration on large-scale data in solid tumors. *J Big Data*. 2023;10(1):165.
26. Passarello K, Kurian S, Villanueva V. Endometrial cancer: an overview of pathophysiology, management, and care. *Semin Oncol Nurs*. 2019;35(2):157–65.
27. Terzic M, Aimagambetova G, Kunz J, Bapayeva G, Aitbayeva B, Terzic S, Laganà AS. Molecular basis of endometriosis and endometrial cancer: current knowledge and future perspectives. *Int J Mol Sci*. 2021;22(17):9274.
28. Zhang C, Liu J, Xu D, Zhang T, Hu W, Feng Z. Gain-of-function mutant p53 in cancer progression and therapy. *J Mol Cell Biol*. 2020;12(9):674–87.
29. Liu Y, Su Z, Tavara O, Gu W. Understanding the complexity of p53 in a new era of tumor suppression. *Cancer Cell*. 2024;42(6):946–67.
30. Duffy MJ, Synnott NC, Crown J. Mutant p53 as a target for cancer treatment. *Eur J Cancer*. 2017;83:258–65.
31. Menon SS, Guruvayoorappan C, Sakthivel KM, Rasmi RR. Ki-67 protein as a tumour proliferation marker. *Clin Chim Acta*. 2019;491:39–45.
32. Cidado J, Wong HY, Rosen DM, Cimino-Mathews A, Garay JP, Fessler AG, Rasheed ZA, Hicks J, Cochran RL, Croessmann S, et al. Ki-67 is required for maintenance of cancer stem cells but not cell proliferation. *Oncotarget*. 2016;7(5):6281–93.
33. O'Neill J, Manion M, Schwartz P, Hockenbery DM. Promises and challenges of targeting Bcl-2 anti-apoptotic proteins for cancer therapy. *Biochim Biophys Acta*. 2004;1705(1):43–51.
34. O'Sullivan J, Kothari C, Caron MC, Gagné JP, Jin Z, Nonfoux L, Beneyton A, Coulombe Y, Thomas M, Atalay N, et al. ZNF432 stimulates parylation and inhibits DNA resection to balance PARPi sensitivity and resistance. *Nucleic Acids Res*. 2023;51(20):11056–79.
35. Xu C, Pei D, Liu Y, Yu Y, Guo J, Liu N, Kang Z. Identification of a novel tumor microenvironment prognostic signature for bladder urothelial carcinoma. *Front Oncol*. 2022;12:818860.

36. Li L, Geng Y, Feng R, Zhu Q, Miao B, Cao J, Fei S. The human RNA surveillance factor UPF1 modulates gastric Cancer progression by targeting long Non-Coding RNA MALAT1. *Cell Physiol Biochem*. 2017;42(6):2194–206.

Publisher's note

Springer Nature remains neutral with regard to jurisdictional claims in published maps and institutional affiliations.